European Journal of Medicinal Chemistry 75 (2014) 438–447

Contents lists available at ScienceDirect

European Journal of Medicinal Chemistry

journal homepage: http://www.elsevier.com/locate/ejmech

Original article

# Design and synthesis of thiazole derivatives as potent FabH inhibitors with antibacterial activity

Jing-Ran Li [a,b,1], Dong-Dong Li [a,b,1], Rong-Rong Wang [a,b], Jian Sun [a,b], Jing-Jun Dong [a,b], Qian-Ru Du [a,b], Fei Fang [a,b], Wei-Ming Zhang [a,b,*], Hai-Liang Zhu [a,b,*]

[a] Nanjing Institute for the Comprehensive Utilization of Wild Plant, Nanjing 210042, People's Republic of China
[b] State Key Laboratory of Pharmaceutical Biotechnology, Nanjing University, Nanjing 210093, People's Republic of China

ARTICLE INFO

*Article history:*
Received 19 June 2013
Received in revised form
2 November 2013
Accepted 14 November 2013
Available online 4 December 2013

*Keywords:*
Thiazole derivatives
Antibacterial
FabH
Molecular docking
3D-QSAR

ABSTRACT

Components of fatty acid biosynthetic pathway have been identified as attractive targets for the development of new antibacterial agents. Compounds of series A (**4a**–**4g**) and series B (**5a**–**5g**) were synthesized by the formation of an amine bond between aromatic acid and 4-phenylthiazol-2-amine or 4-(4-bromophenyl)thiazol-2-amine. These thiazole derivatives have evaluated as potent FabH inhibitors. Nineteen compounds (**4b**–**4h, 4k, 4l**, **5a**–**5h, 5k, 5l**) are reported for the first time. Most of the synthesized compounds exhibited antibacterial activity in the MTT assay. The MIC value of these compounds ranged from 1.56 μg/mL to 100 μg/mL. Moreover, the tested compounds also showed FabH inhibition ability with $IC_{50}$ value ranging from 5.8 μM to 48.1 μM. The $IC_{50}$ values are near the MIC values. Compound **5f** has exhibited the best antibacterial and *Escherichia coli* FabH inhibitory activity. Docking simulation and the QSAR study was conducted for learning about binding mode and the relationship between structure and activity.



## 1. Introduction

Saturated fatty acid biosynthesis pathway has emerged as a prime candidate for developing an important and novel antibacterial [1]. The ubiquitous type II fatty acid synthesis system (FAS) in bacteria is not only essential to cell survival, but also exhibits significant differences between bacterial and human fatty acid synthesis, including the organization, the structure of enzymes and their specific roles. As a result, the differences mentioned above make this system be an attractive target for antibacterial drug discovery [3,4]. β-Ketoacyl-acyl carrier protein (ACP) synthase III, also known as FabH or KAS III, plays an important and regulatory role in bacterial FAS [5]. As is well-known, FabH initiates the fatty acid elongation cycles (Fig. 1), and is involved in feedback regulation of biosynthetic pathway *via* product inhibition [6]. In addition, FabH proteins from both Gram-positive and Gram-negative bacteria are highly conserved at the sequence and structural level, while there are no significantly homologous proteins in humans. Moreover, the residues composing the active site are almost invariant in Gram-positive and negative organisms [7]. These attributes suggest that FabH could be a promising target for designing novel antimicrobial drugs with selectivity, low-toxicity, and broad-spectrum antibacterial activity [8,9].

At the moment, the rise and prevalence of multidrug-resistant pathogenic bacteria have brought us challenges which increase the need to create new types of antibacterial agents and expand the bio-utility of old drugs [2]. Thiazoles and their derivatives have attracted continuing interest over the years for their various biological activities [10]. In past years, they have been used for the treatment of allergies [11], hypertension [12], inflammation [13], schizophrenia [14], bacterial [15], HIV infections [16], hypnotics [17], and more recently for the treatment of pain [18,20]. Furthermore, Kitagawa et al. found that thiazole derivatives not only showed potent FabI and FabK inhibitory activity, but also had an antibacterial effect [19].

In view of these findings, we describe here the synthesis of thiazole derivatives containing an amide skeleton as antibacterial agents [21,22]. This thiazole and amide skeleton combination was suggested in an attempt to investigate the inhibitory activity against *Escherichia coli* FabH. The antimicrobial activity against two Gram-negative bacterial strains (*E. coli* and *Pseudomonas aeruginosa*) and two Gram-positive bacterial strains (*Bacillus subtilis* and *Staphylococcus aureus*) of these thiazole derivatives was determined by applying the standard MTT colorimetric method. The

* Corresponding authors. State Key Laboratory of Pharmaceutical Biotechnology, Nanjing University, Nanjing 210093, People's Republic of China. Tel./fax: +86 25 83592672.
*E-mail addresses:* botanyzh@163.com (W.-M. Zhang), zhuhl@nju.edu.cn (H.-L. Zhu).
[1] These two authors equally contribute to this paper.

0223-5234/$ – see front matter © 2013 Elsevier Masson SAS. All rights reserved.
http://dx.doi.org/10.1016/j.ejmech.2013.11.020

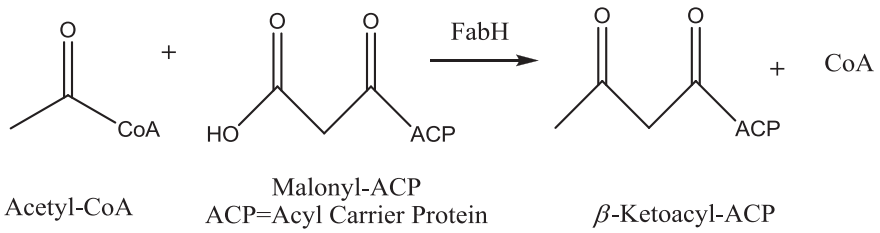


**Fig. 1.** FabH-catalyzed initiation reaction of fatty acid biosynthesis.

antimicrobial activity was shown by the MIC (minimum inhibitory concentrations) values. The enzyme assay was also performed to explore the anti-FabH activity with the selected compounds. Docking simulations were performed using the X-ray crystallographic structure of the FabH of *E. coli* (PDB code: 3IL9) in complex with an inhibitor to explore the binding modes of these compounds at the active site. The structure–activity relationship (SAR) study was also conducted for a better understanding of their activity and their structure relationship using DS 3.5 (Discovery Studio 3.5, Accelrys, Co. Ltd).

## 2. Results and discussion

### 2.1. Chemistry

The synthesis of key intermediates, **3a** and **3b**, is outlined in Scheme 1 [24]. The different substituted α-bromo-acetophenones (**2a**, **2b**) were synthesized by adding bromine ($Br_2$) in the presence of aluminum chloride ($AlCl_3$) as catalyst in THF liquid containing acetophenone or 1-(4-bromophenyl)ethanone. Then, treatment of freshly prepared **2a** or **2b** with thiourea in EtOH produced the 4-phenyl-1,3-thiazol-2-amine (**3a**) and 4-(4-bromo-phenyl)-1,3-thiazol-2-amine (**3b**) in 52% and 47% yields, respectively. Accordingly, the acetyl chloride was synthesized according to Scheme 2. Treatment of **3a** and **3b** with acetyl chloride in acetone in an ice-bath yielded the desired compounds **4a**–**4h** and **5a**–**5h** with moderate to high overall yields. Moreover, as shown in Scheme 3, treatment of the amines, **3a** and **3b**, with benzoic, naphthoic acid or 4-morpholine formic acid in the presence of EDC·HCl and HOBt in $CH_2Cl_2$ yielded the desired compound series **4i**–**4l** and **5i**–**5l**.

### 2.2. Biological activity and molecular modeling

#### 2.2.1. Antibacterial activity and structure–activity relationships analysis

All compounds (**4a**–**4l** and **5a**–**5l**) were screened for antibacterial activity against two Gram-negative bacterial strains: *E. coli*, *P. aeruginosa* and two Gram-positive bacterial strains: *B. subtilis*, *S. aureus* by applying the MTT colorimetric method [26]. The MIC (minimum inhibitory concentrations) values of these compounds were presented in Table 1. Antibacterial agents Kanamycin B and Penicillin G were also screened under identical conditions as positive controls. The results revealed that most synthesized compounds exhibited antibacterial activity with MIC values ranging from 1.56 μg/mL to 100 μg/mL. Among of all the tested twenty-four compounds, fourteen compounds with completed activity information were marked in Table 1. Overall, compounds **4b**, **4e**, **4f**, **5b**, **5e** and **5f** exhibited the greatest antibacterial activity. Particularly, compound **5f** which had MIC values of 1.56, 3.13, 1.56 and 6.25 μg/mL against *E. coli*, *P. aeruginosa*, *B. Subtilis* and *S. aureus*, respectively, and was comparable to the broad-spectrum antibiotic kanamycin B (corresponding MIC: 1.56, 3.13, 0.39 and 3.13 μg/mL) and Penicillin G (corresponding MIC: 3.13, 6.25, 1.56 and 6.25 μg/mL), respectively.

The modification of parent compounds with various substituents such as halogen, methoxyl and ethoxy groups was performed to explore the structure–activity relationships of theses thiazole derivatives. Moreover, we measured the MIC values for each derivative and compared each series (Table 1–3). From Table 2 we found that series B (compounds **5a**–**5g**) showed better antibacterial activity than series A (compounds **4a**–**4g**). The mean values of series B in antibacterial activity against four bacterial strains: *E. coli*, *P. aeruginosa*, *B. subtilis*, and *S. aureus*, were all lower than series A, respectively. What's more, the maximums and minimums of series B in antibacterial activity were also lower than that of series A. This result corresponded directly with their mean values. As shown in Table 3, the total mean value of series A was 29.93 μg/mL and the series B was 14.85 μg/mL, which indicated that series B had better antibacterial activity than series A. The structural difference between these two series confirmed that Br at the *para*-position of the benzene ring was beneficial to the antibacterial activity of the compounds. Still, series A and B both exhibited better activity against Gram-positive bacterial strains compared to Gram-negative bacterial strains. The mean values of series A and B against Gram-positive and Gram-negative bacterial strains were $23.96 < 32.29$ and $11.98 < 17.97$, respectively (Table 3).

Although the compounds of **4h**–**4l**; **5h**–**5l** had ≥100 μg/mL MIC values, we still could conclude that the shorter chain amide group and larger volume acid substituent group at the amide binding sites may be related to their antimicrobial activities. Specifically, compounds **4g**, **4h** and **5h** showed similar moderate antibacterial activity (MIC value: 25–100 μg/mL) against all tested bacterial strains. This indicated that the introduction of a methyl or ethyl (electron-donating group) ether could not enhance the inhibitory activity. Compounds **4i**–**4l** and **5i**–**5l** were found to be inactive against all tested bacterial strains, which indicated that the introduction of morpholine or naphthalene led to the decrease of antibacterial activity. Compound **5g** showed better antibacterial activity than **4g**, which may be due to the Br at the *para*-position of the benzene ring attached to the thiazole ring.

Compared to **4a**, compounds **4b**–**4f** showed more potent antibacterial activity. The MIC values of compound **4a** (25–100 μg/mL) and **4b**–**4f** (3.13–50 μg/mL) suggested that the introduction of halogen substituent at *meta* or *para* position of benzene ring binding with amide could increase antibacterial activity. In addition, for substituent, at the *para* position of the benzene ring of the

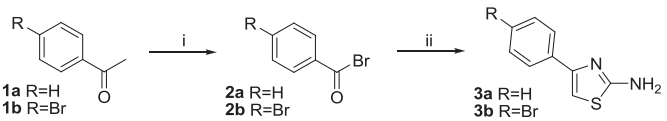


**Scheme 1.** Synthesis of **3a** and **3b**. Reagents and conditions: (i) $Br_2$, $AlCl_3$, THF, 0 °C; (ii) thiourea, EtOH, reflux.

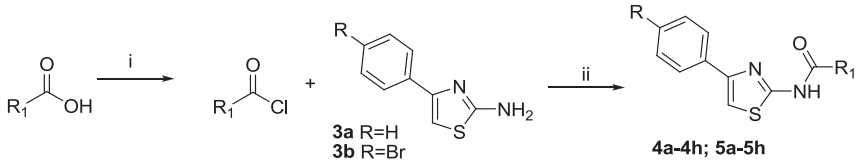


| Compounds | R | $R_1$ | Compounds | R | $R_1$ |
|---|---|---|---|---|---|
| **4a** | H | | **5a** | Br | |
| **4b** | H | | **5b** | Br | |
| **4c** | H | | **5c** | Br | |
| **4d** | H | | **5d** | Br | |
| **4e** | H | | **5e** | Br | |
| **4f** | H | | **5f** | Br | |
| **4g** | H | | **5g** | Br | |
| **4h** | H | | **5h** | Br | |

**Scheme 2.** Synthesis of **4a**–**4h**; **5a**–**5h**. Reagents and conditions: (i) $SOCl_2$, 70–80 °C, reflux, 3 h; (ii) acetone/$K_2CO_3$, ice-bath, reflux for 5 h.

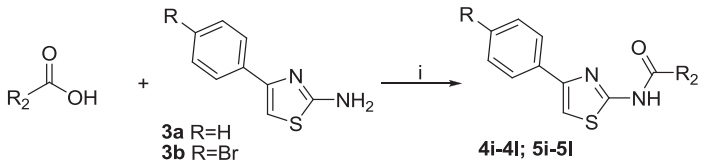


| Compounds | R | $R_2$ | Compounds | R | $R_2$ |
|---|---|---|---|---|---|
| **4i** | H | | **5i** | Br | |
| **4j** | H | | **5j** | Br | |
| **4k** | H | | **5k** | Br | |
| **4l** | H | | **5l** | Br | |

**Scheme 3.** Synthesis of **4i**–**4l**; **5i**–**5l**. Reagents and conditions: (i) acid, EDC, HOBt, $CH_2Cl_2$, RT.

amide, the antibacterial activity of these compounds was slightly enhanced in the following order: Br < Cl < F. The comparison between **5a** and **5b**–**5f** was similar to the example of **4a** and **4b**–**4f**. More interestingly, compounds with substituents at the *para* position of the benzene ring of the amide had less antibacterial activity than those at *meta*-position, which could be seen from the comparison: **4b** > **4e**, **4c** > **4f**; **5b** > **5e**, **5c** > **5f**. This indicated that the location of the substituent also had an influence on the

**Table 1**
MIC (minimum inhibitory concentrations) (μg/mL) values of the synthesized compounds.

| Compounds | Microorganisms[a] | | | |
|---|---|---|---|---|
| | Gram-negative | | Gram-positive | |
| | *E. coli* ATCC35218 | *P. aeruginosa* ATCC13525 | *B. subtilis* ATCC6633 | *S. aureus* ATCC6538 |
| **4a**[b] | 100 | 100 | 50 | 25 |
| **4b**[b] | 12.5 | 25 | 12.5 | 12.5 |
| **4c**[b] | 25 | 25 | 12.5 | 25 |
| **4d**[b] | 50 | 50 | 25 | 50 |
| **4e**[b] | 6.25 | 6.25 | 12.5 | 6.25 |
| **4f**[b] | 12.5 | 12.5 | 6.25 | 3.13 |
| **4g**[b] | 50 | 25 | 100 | 50 |
| **4h** | 50 | 50 | >100 | >100 |
| **4i** | >100 | >100 | >100 | >100 |
| **4j** | >100 | >100 | >100 | >100 |
| **4k** | >100 | >100 | 50 | >100 |
| **4l** | >100 | >100 | >100 | >100 |
| **5a**[c] | 50 | 50 | 25 | 25 |
| **5b**[c] | 12.5 | 12.5 | 6.25 | 12.5 |
| **5c**[c] | 12.5 | 25 | 12.5 | 12.5 |
| **5d**[c] | 25 | 50 | 25 | 25 |
| **5e**[c] | 6.25 | 12.5 | 6.25 | 3.13 |
| **5f**[c] | 1.56 | 3.13 | 1.56 | 6.25 |
| **5g**[c] | 12.5 | 3.13 | 6.25 | 3.13 |
| **5h** | 50 | 25 | 50 | >100 |
| **5i** | >100 | >100 | >100 | >100 |
| **5j** | 50 | 100 | >100 | >100 |
| **5k** | >100 | >100 | >100 | >100 |
| **5l** | 50 | >100 | 100 | >100 |
| Kanamycin B[d] | 1.56 | 3.13 | 0.39 | 3.13 |
| Penicillin G[d] | 3.13 | 6.25 | 1.56 | 6.25 |

[a] Bacterial strains were kindly supplied by State Key Laboratory of Pharmaceutical Biotechnology, Nanjing University.
[b] Compounds **4a**–**4g** were belonged to series A.
[c] Compounds **5a**–**5g** were belonged to series B.
[d] Used as a positive control.

**Table 2**
The mean MIC (minimum inhibitory concentrations) (μg/mL) values of the tested four bacterial strains.

| Series and value | | *E. coli* ATCC35218 | *P. aeruginosa* ATCC13525 | *B. subtilis* ATCC6633 | *S. aureus* ATCC6538 |
|---|---|---|---|---|---|
| Series A[a] | Aver[c] | 28.75 | 26.25 | 22.5 | 23.75 |
| | Mini[c] | 12.5 | 12.5 | 6.25 | 3.13 |
| | Max[c] | 100 | 100 | 100 | 50 |
| Series B[b] | Aver | 11.876 | 20.626 | 11.25 | 11.876 |
| | Mini | 1.56 | 3.13 | 1.56 | 3.13 |
| | Max | 50 | 50 | 25 | 25 |

[a] Series A comprise compounds **4a**–**4g**.
[b] Series B comprise compounds **5a**–**5g**.
[c] Aver represent average value, mini represent minimum value, max represent maximum value. The minimum value and maximum value are excluded from the average value calculation.

**Table 3**
The mean MIC (minimum inhibitory concentrations) (μg/mL) values of Gram-negative and Gram-positive bacterial strains with the total mean values.

| Series[a] | Gram-negative | | | Gram-positive | | | Total | | |
|---|---|---|---|---|---|---|---|---|---|
| | Aver[b] | Mini[b] | Max[b] | Aver | Mini | Max | Aver | Mini | Max |
| A | 32.29 | 12.5 | 100 | 23.96 | 3.13 | 100 | 29.93 | 3.13 | 100 |
| B | 17.97 | 1.56 | 50 | 11.98 | 1.56 | 25 | 14.85 | 1.56 | 50 |

[a] Series A comprise compounds **4a**–**4g**; Series B comprise compounds **5a**–**5g**.
[b] Aver represent average value, mini represent minimum value, max represent maximum value. The minimum value and maximum value are excluded from the average value calculation.

antibacterial activity. So, the compounds of series B with halogen substituent could be the potential antibacterials.

### 2.2.2. *E. coli* FabH inhibitory activity and QSAR study

The *E. coli* FabH inhibitory activity of some thiazole derivatives containing an amide skeleton (**4b**, **4c**, **4e**, **4f**, **4i** and **5b**–**5g**, **5i**) are examined and the results were summarized in Table 4. The CDOCKER_INTERACTION_ENERGY values of these compounds calculated with DS 3.5 (Discovery Studio 3.5, Accelrys, Co. Ltd) are shown in Fig. 2 [25,27]. The lower value indicates better stability of the interaction FabH protein complex (PDB code: 3IL9). The colored dots represent the tested compounds in *E. coli* FabH inhibitory activity assay in Fig. 2. Most of the tested compounds displayed *E. coli* FabH inhibitory activity. Compounds **5b**–**5g** with substituent on the benzene ring located at the C4 position of the thiazole ring showed better *E. coli* FabH inhibitory activity than compounds **4b**, **4c**, **4e** and **4f** which had no substituent on this ring. Another comparison of **5c** and **5e**, **5d** and **5f**, respectively, also indicated that compounds with *m*-substituted Cl or Br located at the benzene ring attached to the amide exhibited better inhibitory activity than those compounds with *p*-substituents. In addition, inactive compounds **4i** and **5i** had no detectable FabH inhibitory activity ($IC_{50}$ > 100 μM). However, in Fig. 2, we found that the CDOCKER_INTERACTION_ENERGY values of compounds **4i** (−49.56) and **5i** (−57.08) were at a tolerated level. Thus the lack of inhibitory activity displayed by these two compounds may be caused by some other reasons, such as poor permeability and solubility.

These $IC_{50}$ values with *E. coli* FabH were correlated with their antibacterial activities. Just as discussed in Tables 1 and 2, series B showed better antibacterial activity than series A. Compounds **4b**, **4f**, **5b**, **5e** and **5f** exhibited the greatest antibacterial and FabH inhibitory activity. This demonstrated that the antibacterial activities of the synthesized compounds were likely due to their FabH inhibitory activities. Besides, the CDOCKER_INTERACTION_ENERGY values of these compounds were also at a lower level. Based on above analysis, some compounds could be the potential antibacterials, especially **5f**, which exhibited the greatest antibacterial and FabH inhibitory activity.

As a supplementary analysis, a 3D-QSAR study was performed by means of the DS 3.5 software (Discovery Studio 3.5, Accelrys, Co. Ltd), aiming for further exploration of structure and activity relationships of these compounds. The 3D-QSAR model was created with the corresponding $pIC_{50}$ values which obtained from the $IC_{50}$ (μM) values of FabH protein inhibition. The $pIC_{50}$ values were derived from an online calculator developed from an Indian medicinal chemistry lab (http://www.sanjeevslab.org/tools-IC50.html) [23]. The observed and predicted values with corresponding residual values in 3D-QSAR model of the training set and test set molecules were listed in Table 5. For a further step, a graphical relationship of the observed $pIC_{50}$ values versus the predicted values is shown in Fig. 3. The linear $R^2$ value was 0.751.

As shown in Fig. 4, the potent compounds containing an electron-withdrawing atom and small substituents not only circumvent the red (in the web version) subregion but also get more close to the favorable yellow spaces. This reference figure displayed that these small molecules could have favorable electrostatic interactions with the protein with minimal steric clashes. This QSAR study could predict that electron-withdrawing atom and small substituents located at the benzene ring may enhance binding affinity of the thiazole derivatives.

### 2.2.3. *Binding model of **5f** and Penicillin G with FabH protein complex*

In order to gain better understanding of the correlations between binding model and biological activity, a docking study was

**Table 4**
*E. coli* FabH inhibitory activity, CDOCKER_INTERACTION_ENERGY and Macrophage CC50 values.

| Compounds | *E. coli* FabH $IC_{50}$ (μM) | CDOCKER_INTERACTION_ENERGY (kcal/mol) | Macrophage CC50 SD (μM) |
|---|---|---|---|
| **4b** | 38.4 ± 0.41 | −42.7372 | 318.4 ± 27.44 |
| **4c** | 41.8 ± 0.38 | −47.8179 | 357.1 ± 33.71 |
| **4e** | 12.3 ± 0.15 | −43.5665 | 264.2 ± 21.43 |
| **4f** | 26.9 ± 0.33 | −41.9839 | 256.8 ± 24.37 |
| **4i** | >100 | −49.5635 | [a]NA |
| **5b** | 29.3 ± 0.31 | −43.5641 | 264.3 ± 27.82 |
| **5c** | 34.7 ± 0.39 | −49.6976 | 285.7 ± 26.58 |
| **5d** | 48.1 ± 0.44 | −50.3613 | 314.9 ± 28.78 |
| **5e** | 9.3 ± 0.17 | −46.7522 | 193.6 ± 27.44 |
| **5f** | 5.8 ± 0.24 | −52.532 | 219.5 ± 21.43 |
| **5g** | 6.6 ± 0.11 | −53.435 | 192.3 ± 19.01 |
| **5i** | >100 | −57.0833 | NA |
| Penicillin G | 4.9 ± 0.13 | −61.7367 | 228.9 ± 20.43 |

Note: the experiment for *E. coli* FabH inhibitory activity repeats 3 times.
[a] NA: not assayed.

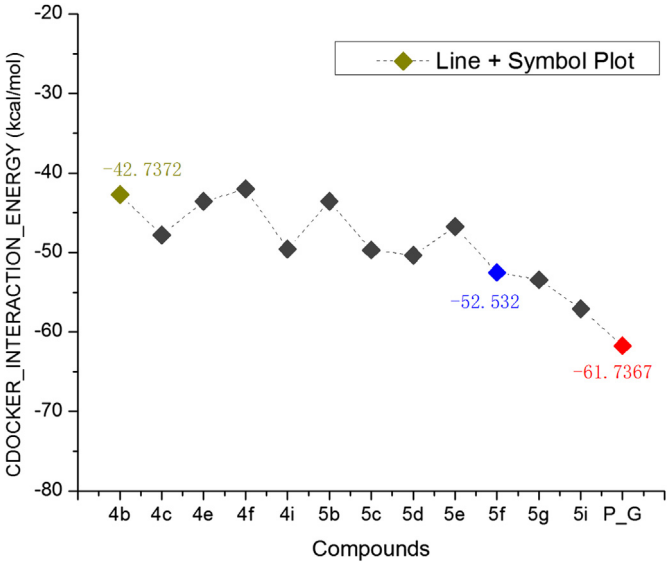


**Fig. 2.** The CDOCKER_INTERACTION_ENERGY (kcal/mol) obtained from the docking study (Discovery Studio 3.5, Accelrys, Co. Ltd).

performed by fitting compound **5f** or Penicillin G into the active site of *E. coli* FabH (PDB code: 3IL9). The binding model of compound **5f** and Penicillin G with FabH protein are depicted in Figs. 5 and 6. In Fig. 5, the 2D projection drawing of compound **5f** or Penicillin G with FabH shows that the two small molecular ligands both fit into

**Table 5**
Experimental, predicted inhibitory activity of compounds **4b**, **4c**, **4e**, **4f** and **5b**–**5g** against *E. coli* FabH protein by 3D-QSAR model.

| Compounds | *E. coli* FabH protein | | Residue value |
|---|---|---|---|
| | Actual $pIC_{50}$ | Predicted $pIC_{50}$ | |
| **4b** | 4.42 | 4.50086 | −0.08086 |
| **4c** | 4.38 | 4.36322 | 0.016781 |
| **4e** | 4.91 | 4.96114 | −0.05114 |
| **4f** | 4.57 | 4.53882 | 0.031179 |
| **5b** | 4.53 | 4.48553 | 0.044468 |
| **5c** | 4.46 | 4.51869 | −0.05869 |
| **5d** | 4.32 | 4.75605 | −0.43605 |
| **5e** | 5.27 | 5.26691 | 0.003093 |
| **5f** | 5.01 | 4.9519 | 0.058096 |
| **5g** | 5.25 | 5.26929 | −0.01929 |

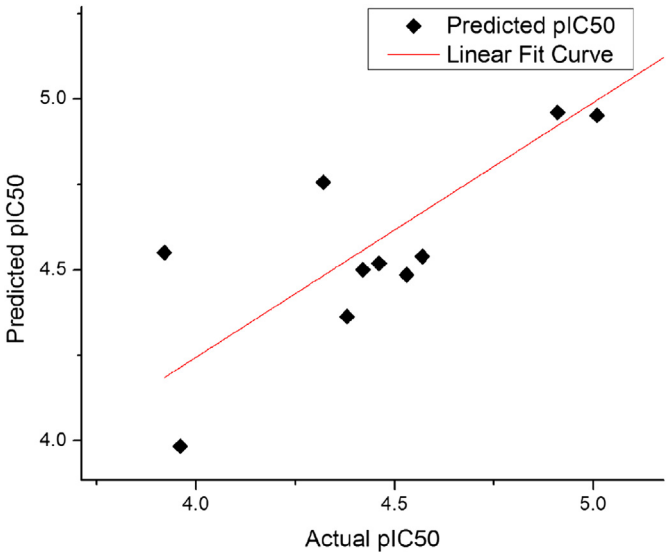


**Fig. 3.** Linear fit curve of the observed $pIC_{50}$ values versus the predicted values of the training set part and the test set part.

the binding site well. The binding model of **5f** in Fig. 6 was the active site of the *E. coli* FabH protein had two Pi-cation and one hydrogen bond. The thiazole ring and benzene ring formed two Pi-cation bond (Pi–N: 5.9 Å; Pi–N: 5.4 Å) with the nitrogen atom of Arg36 and the sulfur-atom locating at the thiazole ring formed a hydrogen bond (S···H–N: 2.2 Å) with the hydrogen atom of Asn247. The two amino acid residues Arg36 and Asn247 located in the binding pocket could be indispensable for the active conformation of the compounds. Though **5f** had a different binding mode with the *E. coli* FabH protein than Penicillin G, it exhibited stabilizing binding interactions with the receptor.

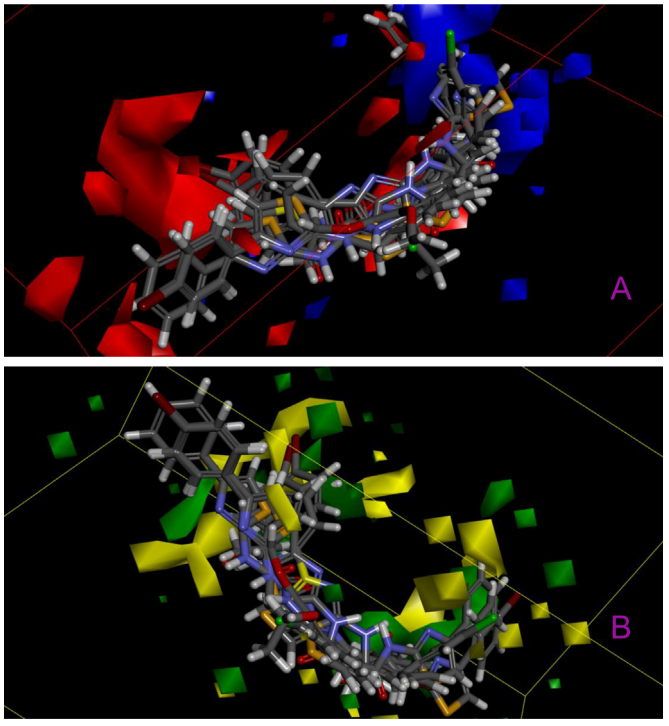


**Fig. 4.** Isosurface of the 3D-QSAR model coefficients.

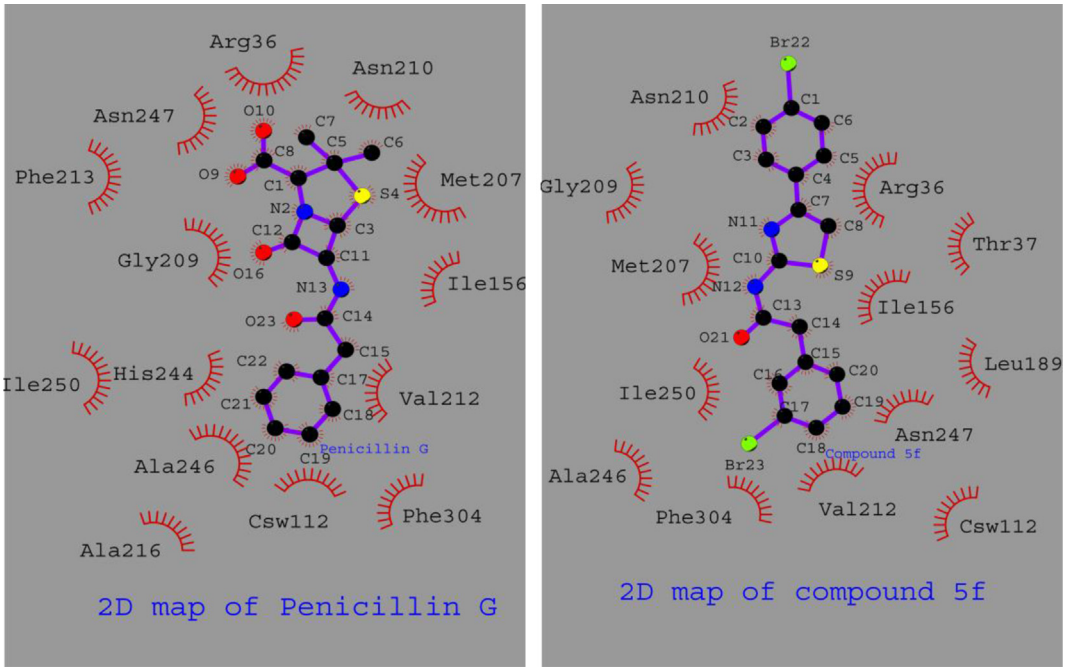


**Fig. 5.** The 2D map of Penicillin G and compound **5f**.

*2.2.4. Cytotoxic*

Compounds were evaluated for their toxicity against human macrophage with the median cytotoxic concentration (CC50) data of tested compounds by the MTT assay. As showed in Table 4, these compounds were tested at multiple doses to study the viability of macrophage. The results showed that they almost did not exhibit cytotoxic activity.

## 3. Conclusion

A series of novel thiazole derivatives containing an amide skeleton were synthesized and their antibacterial activities against *E. coli*, *P. aeruginosa*, *B. Subtilis* and *S. aureus* were also assayed by applying standard MTT colorimetric method. Some compounds showed moderate antibacterial activities that were generally consistent with their potencies as FabH inhibitors. In particular, compound **5f** was the most potent one with an MIC of 1.56–6.25 μg/mL against the tested bacterial strains, which was comparable to the positive control Kanamycin B and Penicillin G. It also exhibited the best *E. coli* FabH inhibitory activity with $IC_{50}$ of 5.8 μM. The enzyme assay data and the molecular docking results suggest that compound **5f** as a potential inhibitor of *E. coli* FabH protein. This study reports compounds with thiazole frameworks containing an amide skeleton may serve as model compounds for the design and development of antibacterial agents. Preliminary structure–activity relationships (3D-QSAR) and molecular modeling study provide further insight into the interactions between FabH and these compounds.

## 4. Experimental

*4.1. General*

All commercially available reagents were obtained from various producers and used without further purification. The reactions were monitored and the purity of the compounds was checked by thin layer chromatography (TLC) using aluminum sheets with Silica Gel 60 $F_{254}$ (Merck). Melting points (uncorrected) were determined on a XT4MP apparatus (Taike Corp., Beijing, China). ESI mass spectra were obtained on a Mariner System 5304 mass spectrometer, and $^1$H NMR spectra were recorded on a Bruker DPX300 spectrometer at 25 °C with TMS and solvent signals allotted as internal standards. Chemical shifts were reported in ppm ($\delta$). Elemental analyses were performed on a CHN–O-Rapid instrument and were within ±0.4% of the theoretical values.

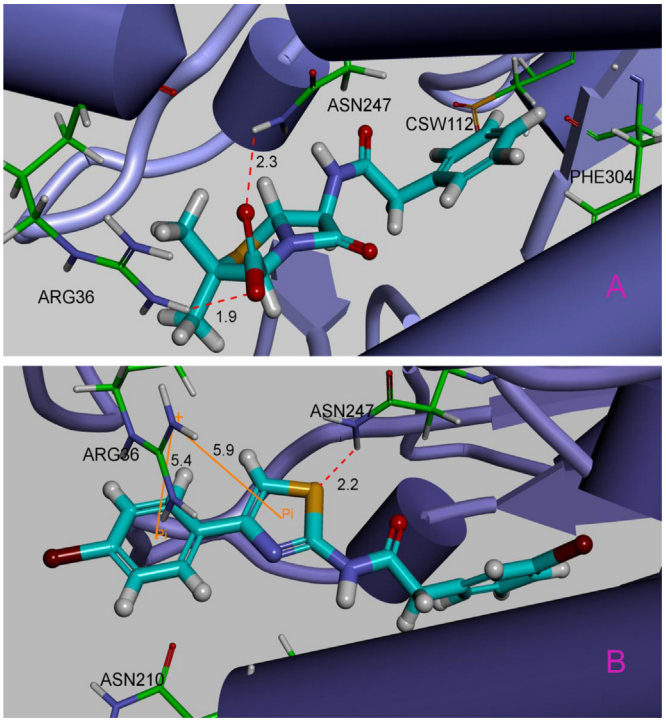


**Fig. 6.** The binding modes of the complexes.

### 4.2. Chemistry synthesis procedure

#### 4.2.1. General procedure for the synthesis of 4-phenylthiazol-2-amine derivatives **3a**, **3b**

Just as outlined in Scheme 1, the compound **1a** (20 mmol) or **1b** (20 mmol) and catalytic amount of $AlCl_3$ was added to a three-necked flask containing THF (40 mL). Then the mixture was cooled to 0 °C and $Br_2$ (20 mmol) stored in the constant pressure funnel was slowly and cautiously added to the mixture in 20 min. After the dropwise add completed, the mixture was evaporated under reduced pressure immediately. Then, precipitation crystallization was washed with mixed solvent of water and petroleum ether to get **2a**, **2b**. Freshly prepared **2a** (20 mmol) or **2b** (20 mmol) and thiourea (22 mmol) in anhydrous EtOH (30 mL) was refluxed for 30 min. After that, the solvent was evaporated under reduced pressure and then the saturated aqueous $NaHCO_3$ was added to make the mixture basic (pH 8–9). Then the mixture was extracted with $CH_2Cl_2$ (3 × 30 mL). The combined organic phases were dried with anhydrous $Na_2SO_4$. After removal of all the solvent, the residue was purified by recrystallization from anhydrous EtOH to afford product **3a** or **3b**, 91% and 93%, respectively.

#### 4.2.2. General procedure for the synthesis of acetamide derivatives **4a**–**4h** and **5a**–**5h**

For the synthesis of compounds **4a**–**4h** and **5a**–**5h** was depicted in Scheme 2. Firstly, 2-phenylacetic acid (1 mmol) and $SOCl_2$ (4–6 mL) were refluxed at 80 °C for 3 h. The reaction liquid was cooled to room temperature and then evaporated to give reactive acyl chloride. The product was obtained as an oil matter, which would be dissolved in acetone (5–6 mL) in the next step. Treatment of **3a** (5-phenylthiazol-2-amine) with 2-phenylacetyl chloride in acetone for 5 h at ice-bath afforded the aimed amine. Meanwhile, $K_2CO_3$ (0.8 g) was added to the mixture. Then the mixture was evaporated under reduced pressure and the resulting solid was washed with diluted NaOH liquid. The aimed amide was extracted from the NaOH liquid with ethyl acetate for column chromatography. Column chromatography was performed using silica gel (200–300 mesh) eluting with ethyl acetate and petroleum ether to give the aimed amine (**4a**). Compounds of **4b**–**4h** and **5a**–**5h** could be got with corresponding acids by the procedures above.

#### 4.2.3. General procedure for the synthesis of acetamide derivatives **4i**–**4l** and **5i**–**5l**

The key intermediates **3a** or **3b** (1 mmol), corresponding acids (1 mmol) and carbodiimide hydrochloride (EDC·HCl, 1.5 mmol) and *N*-hydroxybenzotriazole (HOBt, 0.05 mmol) were stirred in $CH_2Cl_2$ (20–30 mL) at room temperature for 24 h. After that, the solvent was evaporated under reduced pressure to afford a residue, which was extracted with EtOAc (3 × 20 mL). The combined organic phases were dried with anhydrous $Na_2SO_4$. Removal of all the solvent under reduced pressure distillation to get the residue, which was purified with recrystallization to give target products **4i**–**4l** and **5i**–**5l**.

#### 4.2.4. 2-Phenyl-N-(4-phenylthiazol-2-yl)acetamide (**4a**)

White crystal. Yield, 78%. Mp 160–161 °C. $^1$H NMR (300 MHz, $CDCl_3$): $\delta$ 3.81 (s, 2H, $CH_2$), 7.12 (s, 1H), 7.28–7.33 (m, 3H), 7.36–7.44 (m, 5H), 7.76 (d, $J$ = 8.04 Hz, 2H), 8.85 (s, 1H). MS (ESI): 294.1 ($C_{17}H_{14}N_2OS$, $[M + H]^+$). Anal. Calcd for $C_{17}H_{13}N_2OS$: C, 69.36; H, 4.79; N, 9.52. Found: C, 69.03; H, 4.48; N, 9.85%.

#### 4.2.5. 2-(4-Fluorophenyl)-N-(4-phenylthiazol-2-yl)acetamide (**4b**)

Colorless crystal. Yield, 70%. Mp 189–190 °C. $^1$H NMR (300 MHz, $CDCl_3$): $\delta$ 3.77 (s, 2H, $CH_2$), 7.06–7.13 (m, 3H), 7.30–7.34 (m, 3H), 7.39 (t, $J$ = 7.5 Hz, 2H), 7.71 (d, $J$ = 6.96 Hz, 2H), 8.89 (s,1H). MS (ESI): 312.1 ($C_{17}H_{13}FN_2OS$, $[M + H]^+$). Anal. Calcd for $C_{17}H_{12}FN_2OS$: C, 65.37; H, 4.19; N, 8.97. Found: C, 65.73; H, 4.48; N, 8.61%.

#### 4.2.6. 2-(4-Chlorophenyl)-N-(4-phenylthiazol-2-yl)acetamide (**4c**)

Pink crystal. Yield, 73%. Mp 199–200 °C. $^1$H NMR (300 MHz, $CDCl_3$): $\delta$ 3.68 (s, 2H, $CH_2$), 7.16 (t, $J$ = 6.03 Hz, 3H), 7.32–7.42 (m, 5H), 7.8 (d, $J$ = 7.14 Hz, 2H), 9.29 (s, 1H). MS (ESI): 328.1 ($C_{17}H_{13}ClN_2OS$, $[M + H]^+$). Anal. Calcd for $C_{17}H_{12}ClN_2OS$: C, 62.10; H, 3.98; N, 8.52. Found: C, 62.43; H, 3.59; N, 8.75%.

#### 4.2.7. 2-(4-Bromophenyl)-N-(4-phenylthiazol-2-yl)acetamide (**4d**)

Pink crystal. Yield, 68%. Mp 200–201 °C. $^1$H NMR (300 MHz, $CDCl_3$): $\delta$ 3.64 (s, 2H, $CH_2$), 7.1 (d, $J$ = 8.4 Hz, 2H), 7.14 (s, 1H), 7.30–7.35 (m, 1H), 7.40 (t, $J$ = 7.5 Hz, 2H), 7.49 (d, $J$ = 6.42 Hz, 2H), 7.78 (d, $J$ = 6.96 Hz, 2H), 9.37 (s, 1H). MS (ESI): 372.0 ($C_{17}H_{13}BrN_2OS$, $[M + H]^+$). Anal. Calcd for $C_{17}H_{12}BrN_2OS$: C, 54.70; H, 3.51; N, 7.50. Found: C, 54.91; H, 3.22; N, 7.22%.

#### 4.2.8. 2-(3-Chlorophenyl)-N-(4-phenylthiazol-2-yl)acetamide (**4e**)

Colorless crystal. Yield, 75%. Mp 180–181 °C. $^1$H NMR (300 MHz, $CDCl_3$): $\delta$ 3.73 (s, 2H, $CH_2$), 7.14–7.18 (m, 2H), 7.28–7.35 (m, 4H), 7.40 (t, $J$ = 7.68 Hz, 2H), 7.77 (d, $J$ = 7.14 Hz, 2H), 9.14 (s, 1H). MS (ESI): 328.0 ($C_{17}H_{13}ClN_2OS$, $[M + H]^+$). Anal. Calcd for $C_{17}H_{12}ClN_2OS$: C, 62.10; H, 3.98; N, 8.52. Found: C, 62.31; H, 3.69; N, 8.74%.

#### 4.2.9. 2-(3-Bromophenyl)-N-(4-phenylthiazol-2-yl)acetamide (**4f**)

Colorless crystal. Yield, 68%. Mp 183–184 °C. $^1$H NMR (300 MHz, $CDCl_3$): $\delta$ 3.73 (s, 2H, $CH_2$), 7.14 (s, 1H), 7.18–7.24 (m, 2H), 7.31–7.48 (m, 5H), 7.77 (d, $J$ = 6.93 Hz, 2H), 9.57 (s, 1H). MS (ESI): 372.0 ($C_{17}H_{13}BrN_2OS$, $[M + H]^+$). Anal. Calcd for $C_{17}H_{12}BrN_2OS$: C, 54.70; H, 3.51; N, 7.50. Found: C, 54.99; H, 3.82; N, 7.81%.

#### 4.2.10. 2-(3-Methoxyphenyl)-N-(4-phenylthiazol-2-yl)acetamide (**4g**)

Pink crystal. Yield, 56%. Mp 99–101 °C. $^1$H NMR (300 MHz, $CDCl_3$): $\delta$ 3.76 (s, 2H, $CH_2$), 3.84 (s, 3H), 6.59 (s, 1H), 6.81–6.89 (m, 3H), 7.11 (s, 1H), 7.42–7.47 (m, 3H), 7.72 (d, $J$ = 8.04 Hz, 2H), 8.60 (s, 1H). MS (ESI): 324.1 ($C_{18}H_{16}N_2O_2S$, $[M + H]^+$). Anal. Calcd for $C_{18}H_{15}N_2O_2S$: C, 66.64; H, 4.97; N, 8.64. Found: C, 66.99; H, 4.66; N, 8.37%.

#### 4.2.11. 2-(3,4-Diethoxyphenyl)-N-(4-phenylthiazol-2-yl)acetamide (**4h**)

White crystal. Yield, 58%. Mp 116–118 °C. $^1$H NMR (300 MHz, $CDCl_3$): $\delta$ 1.43–1.49 (m, 6H), 3.72 (s, 2H, $CH_2$), 4.05–4.15 (m, 4H), 6.80 (d, $J$ = 6.96 Hz, 2H), 6.89 (d, $J$ = 8.76 Hz, 1H), 7.12 (s, 1H), 7.28–7.31 (m, 1H), 7.32–7.42 (m, 2H), 7.76 (d, $J$ = 7.14 Hz, 2H), 8.93 (s, 1H). MS (ESI): 382.1 ($C_{21}H_{22}N_2O_3S$, $[M + H]^+$). Anal. Calcd for $C_{21}H_{21}N_2O_3S$: C, 65.95; H, 5.80; N, 7.32. Found: C, 65.59; H, 5.51; N, 7.65%.

#### 4.2.12. N-(4-Phenylthiazol-2-yl)benzamide (**4i**)

Yellow crystal. Yield, 84%. Mp 85–86 °C. $^1$H NMR (300 MHz, $CDCl_3$): $\delta$ 7.20 (s, 1H), 7.31–7.36 (m, 1H), 7.42 (t, $J$ = 7.14 Hz, 2H), 7.53 (t, $J$ = 6.78 Hz, 2H), 7.60–7.64 (m, 1H), 7.83 (d, $J$ = 6.96 Hz, 2H), 7.97 (d, $J$ = 8.43 Hz, 2H), 9.89 (s, 1H). MS (ESI): 280.1 ($C_{16}H_{12}N_2OS$, $[M + H]^+$). Anal. Calcd for $C_{16}H_{11}N_2OS$: C, 68.55; H, 4.31; N, 9.99. Found: C, 68.23; H, 4.62; N, 9.66%.

#### 4.2.13. N-(4-Phenylthiazol-2-yl)-1-naphthamide (**4j**)

Colorless crystal. Yield, 62%. Mp 178–180 °C. $^1$H NMR (300 MHz, $CDCl_3$): $\delta$ 7.22 (s, 1H), 7.32–7.37 (m, 1H), 7.41–7.46 (m, 2H), 7.83 (d, $J$ = 6.96 Hz, 2H), 7.89–7.97 (m, 3H), 8.06 (d, $J$ = 8.22 Hz, 2H), 8.34 (d, $J$ = 7.32 Hz, 1H), 8.55 (d, $J$ = 8.25 Hz, 1H), 8.89 (d, $J$ = 8.58 Hz, 1H).

MS (ESI): 330.1 ($C_{20}H_{14}N_2OS$, $[M + H]^+$). Anal. Calcd for $C_{20}H_{13}N_2OS$: C, 72.70; H, 4.27; N, 8.48. Found: C, 72.96; H, 4.48; N, 8.79%.

*4.2.14. N-(4-Phenylthiazol-2-yl)-2-naphthamide (**3k**)*

Colorless crystal. Yield, 64%. Mp 168–169 °C. $^1$H NMR (300 MHz, $CDCl_3$): δ 7.22 (s, 1H), 7.30–7.35 (m, 1H), 7.40–7.44 (m, 2H), 7.58–7.67 (m, 2H), 7.85 (d, $J$ = 6.96 Hz, 2H), 7.91–7.97 (m, 2H), 7.99 (s, 2H), 8.50 (s, 1H). MS (ESI): 330.1 ($C_{20}H_{14}N_2OS$, $[M + H]^+$). Anal. Calcd for $C_{20}H_{13}N_2OS$: C, 72.70; H, 4.27; N, 8.48. Found: C, 72.39; H, 4.47; N, 8.60%.

*4.2.15. N-(4-Phenylthiazol-2-yl)morpholine-4-carboxamide (**4l**)*

Yellow crystal. Yield, 88%. Mp 155–156 °C. $^1$H NMR (300 MHz, $CDCl_3$): δ 3.76–3.78 (m, 8H), 7.02 (s, 1H), 7.47–7.54 (m, 3H), 7.75 (d, $J$ = 6.48 Hz, 2H), 9.44 (s, 1H). MS (ESI): 389.1 ($C_{14}H_{15}N_3O_2S$, $[M + H]^+$). Anal. Calcd for $C_{14}H_{14}N_3O_2S$: C, 58.11; H, 5.23; N, 14.52. Found: C, 58.49; H, 5.42; N, 14.25%.

*4.2.16. N-(4-(4-Bromophenyl)thiazol-2-yl)-2-phenylacetamide (**5a**)*

Pink crystal. Yield, 80%. Mp 210–211 °C. $^1$H NMR (300 MHz, $CDCl_3$): δ 3.84 (s, 2H, $CH_2$), 7.12 (s, 1H), 7.32–7.43 (m, 5H), 7.50 (d, $J$ = 8.76 Hz, 2H), 7.64 (d, $J$ = 8.76 Hz, 2H), 8.67 (s, 1H). MS (ESI): 372.0 ($C_{17}H_{13}BrN_2OS$, $[M + H]^+$). Anal. Calcd for $C_{17}H_{12}BrN_2OS$: C, 54.70; H, 3.51; N, 7.50. Found: C, 54.96; H, 3.72; N, 7.89%.

*4.2.17. N-(4-(4-Bromophenyl)thiazol-2-yl)-2-(4-fluorophenyl) acetamide (**5b**)*

Pink crystal. Yield, 68%. Mp 218–219 °C. $^1$H NMR (300 MHz, $CDCl_3$): δ 3.81 (s, 2H, $CH_2$), 7.11–7.14 (m, 3H), 7.28–7.33 (m, 2H), 7.51 (d, $J$ = 8.61 Hz, 2H), 7.60–7.66 (m, 2H), 8.80 (s, 1H). MS (ESI): 390.0 ($C_{17}H_{12}BrFN_2OS$, $[M + H]^+$). Anal. Calcd for $C_{17}H_{11}BrFN_2OS$: C, 52.19; H, 3.09; N, 7.16. Found: C, 52.56; H, 3.40; N, 6.98%.

*4.2.18. N-(4-(4-Bromophenyl)thiazol-2-yl)-2-(4-chlorophenyl) acetamide (**5c**)*

Yellow crystal. Yield, 70%. Mp 218–219 °C. $^1$H NMR (300 MHz, $CDCl_3$): δ 3.74 (s, 2H, $CH_2$), 7.13 (s, 1H), 7.30 (s, 2H), 7.39 (d, $J$ = 8.4 Hz, 2H), 7.54 (d, $J$ = 8.4 Hz, 2H), 7.64 (d, $J$ = 8.4 Hz, 2H), 9.55 (s, 1H). MS (ESI): 406.0 ($C_{17}H_{12}BrClN_2OS$, $[M + H]^+$). Anal. Calcd for $C_{17}H_{11}BrClN_2OS$: C, 50.08; H, 2.97; N, 6.87. Found: C, 50.36; H, 2.68; N, 7.08%.

*4.2.19. 2-(4-Bromophenyl)-N-(4-(4-bromophenyl)thiazol-2-yl) acetamide (**5d**)*

Pink crystal. Yield, 71%. Mp 211–212 °C. $^1$H NMR (300 MHz, $CDCl_3$): δ 3.78 (s, 2H, $CH_2$), 7.13 (s, 1H), 7.21 (d, $J$ = 8.43 Hz, 2H), 7.53 (t, $J$ = 8.43 Hz, 4H), 7.64 (d, $J$ = 8.61 Hz, 2H), 8.99 (s, 1H). MS (ESI): 450.0 ($C_{17}H_{12}Br_2N_2OS$, $[M + H]^+$). Anal. Calcd for $C_{17}H_{11}Br_2N_2OS$: C, 45.16; H, 2.67; N, 6.20. Found: C, 45.46; H, 2.88; N, 6.02%.

*4.2.20. N-(4-(4-Bromophenyl)thiazol-2-yl)-2-(3-chlorophenyl) acetamide (**5e**)*

Yellow crystal. Yield, 78%. Mp 170–172 °C. $^1$H NMR (300 MHz, $CDCl_3$): δ 3.76 (s, 2H, $CH_2$), 7.14 (s, 1H), 7.17–7.20 (m, 1H), 7.31–7.34 (m, 3H), 7.52 (d, $J$ = 8.61 Hz, 2H), 7.64 (d, $J$ = 8.61 Hz, 2H), 9.23 (s, 1H). MS (ESI): 406.0 ($C_{17}H_{12}BrClN_2OS$, $[M + H]^+$). Anal. Calcd for $C_{17}H_{11}BrClN_2OS$: C, 50.08; H, 2.97; N, 6.87. Found: C, 50.38; H, 2.68; N, 7.09%.

*4.2.21. 2-(3-Bromophenyl)-N-(4-(4-bromophenyl)thiazol-2-yl) acetamide (**5f**)*

Pink crystal. Yield, 65%. Mp 182–183 °C. $^1$H NMR (300 MHz, $CDCl_3$): δ 3.74 (s, 2H, $CH_2$), 7.13 (s, 1H), 7.48–7.54 (m, 5H), 7.64 (d, $J$ = 8.61 Hz, 3H), 9.19 (s, 1H). MS (ESI): 450.0 ($C_{17}H_{12}Br_2N_2OS$, $[M + H]^+$). Anal. Calcd for $C_{17}H_{11}Br_2N_2OS$: C, 45.16; H, 2.67; N, 6.20. Found: C, 45.48; H, 2.88; N, 6.01%.

*4.2.22. N-(4-(4-Bromophenyl)thiazol-2-yl)-2-(3-methoxyphenyl) acetamide (**5g**)*

Pink crystal. Yield, 55%. Mp 112–113 °C. $^1$H NMR (300 MHz, $CDCl_3$): δ 3.71 (s, 2H, $CH_2$), 3.83 (s, 3H), 6.85–6.93 (m, 3H), 7.12 (s, 1H), 7.34 (t, $J$ = 7.86 Hz, 1H), 7.49 (d, $J$ = 6.39 Hz, 2H), 7.63 (d, $J$ = 6.75 Hz, 2H), 8.78 (s, 1H). MS (ESI): 402.0 ($C_{18}H_{15}BrN_2O_2S$, $[M + H]^+$). Anal. Calcd for $C_{18}H_{14}BrN_2O_2S$: C, 53.61; H, 3.75; N, 6.95. Found: C, 53.89; H, 3.45; N, 7.16%.

*4.2.23. N-(4-(4-Bromophenyl)thiazol-2-yl)-2-(3,4-diethoxyphenyl) acetamide (**5h**)*

. White crystal. Yield, 56%. Mp 149–150 °C. $^1$H NMR (300 MHz, $CDCl_3$): δ 1.44–1.50 (m, 6H), 3.76 (s, 2H, $CH_2$), 4.06–4.16 (m, 4H), 6.83 (d, $J$ = 8.97 Hz, 2H), 6.91 (d, $J$ = 7.86 Hz, 1H), 7.11 (s, 1H), 7.50 (d, $J$ = 8.79 Hz, 2H), 7.64 (d, $J$ = 8.58 Hz, 2H), 8.66 (s, 1H). MS (ESI): 460.1 ($C_{21}H_{21}BrN_2O_3S$, $[M + H]^+$). Anal. Calcd for $C_{21}H_{20}BrN_2O_3S$: C, 54.67; H, 4.59; N, 6.07. Found: C, 54.95; H, 4.70; N, 6.29%.

*4.2.24. N-(4-(4-Bromophenyl)thiazol-2-yl)benzamide (**5i**)*

Colorless crystal. Yield, 88%. Mp 120–122 °C. $^1$H NMR (300 MHz, DMSO-$d_6$): δ 7.17 (s, 2H), 7.60–7.62 (m, 4H), 7.71–7.78 (m, 4H), 9.67 (s, 1H). MS (ESI): 358.0 ($C_{16}H_{11}BrN_2OS$, $[M + H]^+$). Anal. Calcd for $C_{16}H_{10}BrN_2OS$: C, 53.49; H, 3.09; N, 7.80. Found: C, 53.76; H, 3.40; N, 7.52%.

*4.2.25. N-(4-(4-Bromophenyl)thiazol-2-yl)-1-naphthamide (**5j**)*

Colorless crystal. Yield, 64%. Mp 150–151 °C. $^1$H NMR (300 MHz, DMSO-$d_6$): δ 7.29 (s, 1H), 7.69–7.74 (m, 4H), 7.79–7.87 (m, 3H), 7.95 (d, $J$ = 8.04 Hz, 2H), 8.11 (d, $J$ = 7.32 Hz, 1H), 8.31 (d, $J$ = 9.69 Hz, 1H), 8.87 (d, $J$ = 8.4 Hz, 1H). MS (ESI): 408.0 ($C_{20}H_{13}BrN_2OS$, $[M + H]^+$). Anal. Calcd for $C_{20}H_{12}BrN_2OS$: C, 58.69; H, 3.20; N, 6.84. Found: C, 58.96; H, 3.49; N, 6.99%.

*4.2.26. N-(4-(4-Bromophenyl)thiazol-2-yl)-2-naphthamide (**5k**)*

Colorless crystal. Yield, 67%. Mp 123–125 °C. $^1$H NMR (300 MHz, $CDCl_3$): δ 7.22 (s, 1H), 7.53 (d, $J$ = 8.58 Hz, 2H), 7.59–7.70 (m, 2H), 7.92–8.04 (m, 4H), 8.20 (d, $J$ = 8.58 Hz, 1H), 8.50 (s, 1H), 8.79 (s, 1H). MS (ESI): 408.0 ($C_{20}H_{13}BrN_2OS$, $[M + H]^+$). Anal. Calcd for $C_{20}H_{12}BrN_2OS$: C, 58.69; H, 3.20; N, 6.84. Found: C, 58.99; H, 3.49; N, 6.53%.

*4.2.27. N-(4-(4-Bromophenyl)thiazol-2-yl)morpholine-4-carboxamide (**5l**)*

White crystal. Yield, 83%. Mp 143–144 °C. $^1$H NMR (300 MHz, DMSO-$d_6$): δ 3.48–3.53 (m, 4H), 3.58–3.60 (m, 4H), 7.03 (s, 1H), 7.42–7.45 (m, 2H), 7.69 (d, $J$ = 8.61 Hz, 2H), 9.58 (s, 1H). MS (ESI): 367.0 ($C_{14}H_{14}BrN_3O_2S$, $[M + H]^+$). Anal. Calcd for $C_{14}H_{13}BrN_3O_2S$: C, 45.66; H, 3.83; N, 11.41. Found: C, 45.89; H, 3.62; N, 11.63%.

### *4.3. Antibacterial activity*

The antibacterial activity of the synthesized compounds was tested against *E. coli*, *P. aeruginosa*, *B. subtilis* and *S. aureus* using MH medium (Muellere–Hinton medium: casein hydrolyzate 17.5 g, soluble starch 1.5 g, beef extract 1000 mL). The MICs (minimum inhibitory concentrations) of the test compounds were determined by a colorimetric method using the dye MTT (3-(4,5-dimethylthiazol-2-yl)-2,5-diphenyl-trtrazolium bromide). A stock solution of the synthesized compound (1 mg/mL) in DMSO was prepared and graded quantities of the test compounds were incorporated in specified quantity of sterilized liquid MH medium.

A specified quantity of the medium containing the compound was poured into microtitration plates. Suspension of the microorganism was prepared to contain approximately $10^5$ cfu/mL and applied to microtitration plates with serially diluted compounds in DMSO to be tested and incubated at 37 °C for 24 h. After the MICs were visually determined on each of the microtitration plates, 50 μL of PBS (Phosphate Buffered Saline 0.01 mol/L, pH 7.4: $Na_2HPO_4 \cdot 12H_2O$ 2.9 g, $KH_2PO_4$ 0.2 g, NaCl l8.0 g, KCl 0.2 g, distilled water 1000 mL) containing 2 mg of MTT/mL was added to each well. Incubation was continued at room temperature for 4–5 h. The content of each well was removed, and 100 μL of isopropanol containing 5% 1 mol/L HCl was added to extract the dye. After 12 h of incubation at room temperature, the opticaldensity (OD) was measured with a microplate reader at 550 nm. The observed MICs were presented in Table 1.

### 4.4. E. coli FabH purification and activity assay

Full-length *E. coli* acyl carrier protein (ACP), acyl carrier protein synthase (ACPS), and β-ketoacyl-ACP synthase III (FabH) were individually cloned into pET expression vectors with an *N*-terminal His-tag (ACP, ACPS in pET 19; FabH in pET 28).

All proteins were expressed in *E. coli* strain BL21 (DE3). Transformed cells were grown on Luria–Bertani (LB) agar plates supplemented with kanamycin (30 μg/mL). Sodium dodecyl sulfate-polyacrylamide gel electrophoresis (SDS-PAGE) analysis was used to screen colonies for overexpression of proteins. One such positive colony was used to inoculate 10 mL of LB medium with 30 μg/mL of kanamycin and grown overnight at 37 °C, 1 mL of which was used to inoculate 100 mL LB medium supplemented with 30 μg/mL of kanamycin. The culture was shaken for 4 h at 37 °C, and then induced with 0.5 mM isopropyl b-D-thio galacto pyranoside (IPTG). The culture was grown for 4 h, and harvested by centrifugation (30 min at 15,000 rpm).

Harvested cells containing His-tagged ACP, ACPS, and FabHs were lysed by sonication in 20 mM Tris, pH 7.6, 5 mM imidazole, 0.5 M NaCl and centrifuged at 20, 000 rpm for 30 min. The supernatant was applied to a Ni–NTA agarose column, washed, and eluted using a 5–500 mM imidazole gradient over 20 column volumes. Eluted protein was dialyzed against 20 mM Tris, pH 7.6, 1 mM DTT, and 100 mM NaCl. Purified FabHs were concentrated up to 2 mg/mL and stored at −80 °C in 20 mM Tris, pH 7.6, 100 mM NaCl, 1 mM DTT, and 20% glycerol for enzymatic assays.

Purified ACP contains the apo-form that needs to be converted into the holo-form. The conversion reaction is catalyzed by ACP synthase (ACPS). In the final volume of 50 mL, 50 mg ACP, 50 mM Tris, 2 mM DTT, 10 mM $MgCl_2$, 600 μM CoA, and 0.2 μM ACPS was incubated for 1 h at 37 °C. The pH of the reaction was then adjusted to approximately 7.0 using 1 M potassium phosphate. Holo-ACP was purified by fractionation of the reaction mixture by Source Q-15 ion exchange chromatography using a 0–500 mM NaCl gradient over 25 column volumes.

In a final 20 μL reaction, 20 mM $Na_2HPO_4/NaH_2PO_4$, pH 7.0, 0.5 mM DTT, 0.25 mM $MgCl_2$, and 2.5 mM holo-ACP were mixed with 1 nM FabH, and $H_2O$ was added to 15 μL. After1 min incubation, a 2 μL mixture of 25 μM acetyl-CoA and 0.75 μCi [$^3$H] acetyl-CoA was added for FabH reaction for 25 min. The reaction was stopped by adding 20 μL of ice-cold 50% TCA, incubating for 5 min on ice, and centrifuging to pellet the protein. The pellet was washed with 10% ice-cold TCA and resuspended with 5 μL of 0.5 M NaOH. The incorporation of the $^3$H signal in the final product was read by liquid scintillation. When determining the inhibition constant ($IC_{50}$), inhibitors were added from a concentrated DMSO stock such that the final concentration of DMSO did not exceed 2%.

### 4.5. Cytotoxicity on human macrophage

The cytotoxicity test of compounds was measured by the colorimetric MTT assay. Human macrophage suspension in DMEM medium supplemented with 10% FBS and 1× antimycotic was added in 96-well microplates at 1.8 × 104 cells/well. Then, various concentrations of the test compounds (160, 40, 10, 2.5, 0.25 μg/mL) dissolved in distilled 10% DMSO (10 μL) was added to each well. After incubation for 24 h at 37 °C under 5% $CO_2$, 2.5 mg/mL of MTT solution (μL) was added to each well. The plate was incubated for a further 4 h. Then, the incubation medium was aspirated, and DMSO (100 μL) was added to solubilize the MTT formazan product. After mixing, the absorbances at 570 and 655 nm were measured. The difference between absorbance at 570 and 630 nm was used as an index of the cell viability. The morphology of the cells was observed using Giemsa stain under Phase contrast microscope. Metronidazole–thiazoles derivatives were used as a positive control, whereas untreated cells were used as negative controls. The concentration of the compound that killed 50% of the cells (CC50) was calculated by GraphPad Prism 4 software. All determinations were performed in triplicate. The results were summarized in Table 4.

### 4.6. Virtual calculation

#### 4.6.1. 3D-QSAR study

Ligand-based 3D-QSAR approach was performed by QSAR software of DS 3.5 (Discovery Studio 3.5, Accelrys, Co. Ltd). The training sets were composed of 6 small molecular while test sets comprised 4 compounds. The corresponding $pIC_{50}$ values were converted from the obtained $IC_{50}$ (nM) (http://www.sanjeevslab.org/tools-IC50.html).[2] All the definition of the descriptors can be seen in the help of DS 3.5 software and they were calculated by QSAR protocol of DS 3.5. The alignment conformation of each molecule was the one with lowest interaction energy in the docked results of CDOCKER.

#### 4.6.2. Molecular docking modeling

The crystal structures of the proteins complex were retrieved from the RCSB Protein Data Bank (http://www.rcsb.org/pdb/home/home.do). The three-dimensional structures of the aforementioned compounds were constructed using Chem. 3D ultra 12.0 software [Chemical Structure Drawing Standard; Cambridge Soft corporation, USA (2010)], then they were energetically minimized by using MMFF94 with 5000 iterations and minimum RMS gradient of 0.10.

Molecular docking of compound **5f** into the three-dimensional *E. coli* FabH protein complex structure (3IL9.pdb, downloaded from the PDB) was carried out using the Discovery Studio (version 3.5) as implemented through the graphical user interface DS-CDOCKER protocol, all bound waters and ligands were eliminated from the protein and the polar hydrogen was added to the proteins.

## Acknowledgments

We thank Miss Zhu Shen in Nanjing Foreign Languages School for the synthesis of compounds **3a** and **3b** of this paper. This work was supported by National Science & Technology Pillar Program during the Twelfth Five-year Plan Period (No. 2012BAD36B01).

[2] The $pIC_{50}$ value calculator is a web tool which is developed by using JavaScript and HTML, to convert $IC_{50}$ to $pIC_{50}$ values. It is available online. To enter this website, the $IC_{50}$ values were input into the calculator surface one by one, and then we got the corresponding $pIC_{50}$ values.

## References


[1] A.C. Price, K.H. Choi, R.J. Heath, Z. Li, S.W. White, C.O. Rock, J. Biol. Chem. 276 (2001) 6551–6559.
[2] M. Leeb, Nature 431 (2004) 892–893.
[3] S.S. Khandekar, D.R. Gentry, G.S. Van Aller, P. Warren, H. Xiang, C. Silverman, M.L. Doyle, P.A. Chambers, A.K. Konstantinidis, M. Brandt, R.A. Daines, J.T. Lonsdale, J. Biol. Chem. 276 (2001) 30024–30030.
[4] X. Qiu, C.A. Janson, W.W. Smith, M. Head, J. Lonsdale, A.K. Konstantinidis, J. Mol. Biol. 307 (2001) 341–356.
[5] S.S. Khandekar, R.A. Daines, J.T. Lonsdale, Curr. Protein Pept. Sci. 4 (2003) 21–29.
[6] R.J. Heath, C.O. Rock, J. Biol. Chem. 271 (1996) 10996–11000.
[7] Z. Nie, C. Perretta, J. Lu, Y. Su, S. Margosiak, K.S. Gajiwala, J. Cortez, V. Nikulin, K.M. Yager, K. Appelt, S. Chu, J. Med. Chem. 48 (2005) 1596–1609.
[8] J. Wang, S. Kodali, S.H. Lee, A. Galgoci, R. Painter, Proc. Natl. Acad. Sci. 104 (2007) 7612–7616.
[9] R.J. Heath, C.O. Rock, Curr. Opin. Investig. Drugs 5 (2004) 146–153.
[10] I. Hutchinson, S.A. Jennings, B.R. Vishnuvajjala, A.D. Westwell, M.F. Stevens, J. Med. Chem. 45 (2002) 744–747.
[11] K.D. Hargrave, F.K. Hess, J.T. Oliver, J. Med. Chem. 26 (1983) 1158–1163.
[12] W.C. Patt, H.W. Hamilton, M.D. Taylor, M.J. Ryan, D.G. Taylor Jr., C.J. Connolly, A.M. Doherty, S.R. Klutchko, I. Sircar, B.A. Steinbaugh, B.L. Batley, C.A. Painchaud, S.T. Rapundalo, B.M. Michniewicz, S.C.J. Olson, J. Med. Chem. 35 (1992) 2562–2572.
[13] P.K. Sharma, D.E. Schuller, J.H. Goodman, S.P. Smith, F.P. Goldman, S. Raj, R.E. Nicholson, D.C. Young, Indian J. Chem. 124 (1998) 149–152.
[14] J.C. Jaen, L.D. Wise, B.W. Caprathe, H. Tecle, S. Bergmeier, C.C. Humblet, T.G. Heffner, L.T. Meltzer, T.A. Pugsley, J. Med. Chem. 33 (1990) 311–317.
[15] K. Tsuji, H. Ishikawa, Bioorg. Med. Chem. Lett. 4 (1994) 1601–1606.
[16] F.W. Bell, A.S. Cantrell, M. Hogberg, S.R. Jaskunas, N.G. Johansson, C.L. Jordan, M.D. Kinnick, P. Lind, J.M. Morin Jr., R. Noreen, B. Oberg, J.A. Palkowitz, C.A. Parrish, P. Pranc, C. Sahlberg, R.J. Ternansky, R.T. Vasileff, L. Vrang, S.J. West, H. Zhang, X.X. Zhou, J. Med. Chem. 38 (1995) 4929–4936.
[17] N. Ergenc, G. Capan, N.S. Gunay, S. Ozkirimli, M. Gungor, S. Ozbey, E. Kendi, Arch. Pharm. Pharm. Med. Chem. 332 (1999) 343–347.
[18] J.S. Carter, S. Kramer, J.J. Talley, T. Penning, P. Collins, M.J. Graneto, K. Seibert, C.M. Koboldt, J. Masferrer, B. Zweifel, Bioorg. Med. Chem. Lett. 9 (1999) 1171–1174.
[19] H. Kitagawa, T. Ozawa, S. Takahata, M. Iida, J. Saito, M. Yamada, J. Med. Chem. 50 (2007) 4710–4720.
[20] Z.C. Wang, Y.T. Duan, Y.J. Qin, P.F. Wang, Y. Luo, Eur. J. Med. Chem. 65 (2013) 456–463.
[21] Y.S. Yang, F. Zhang, C. Gao, Y.B. Zhang, X.L. Wang, J.F. Tang, J. Sun, H.B. Gong, H.L. Zhu, Bioorg. Med. Chem. Lett. 22 (2012) 4619–4624.
[22] P.C. Lv, K.R. Wang, Y. Yang, W.J. Mao, J. Chen, J. Xiong, Bioorg. Med. Chem. Lett. 19 (2009) 6750–6754.
[23] C. Selvaraj, S.K. Tripathi, K.K. Reddy, S.K. Singh, Curr. Trends Biotechnol. Pharm. 5 (2011) 1104–1109.
[24] X.L. Qiu, G. Li, G. Wu, J. Zhu, L. Zhou, P.L. Chen, A.R. Chamberlin, W.H. Lee, J. Med. Chem. 52 (2009) 1757–1767.
[25] G.M. Morris, D.S. Goodsell, R.S. Halliday, R. Huey, W.E. Hart, R.K. Belew, A.J. Olson, J. Comput. Chem. 19 (1998) 1639–1662.
[26] L. Shi, R.Q. Fang, Z.W. Zhu, Y. Yang, K. Cheng, W.Q. Zhong, Hai-Liang Zhu, Eur. J. Med. Chem. 45 (2010) 4358–4364.
[27] R. Huey, G.M. Morris, A.J. Olson, D.S. Goodsell, J. Comput. Chem. 28 (2007) 1145–1152.